

## Numerical Study of Spring Response of 20000TEU Containership in Waves

Fan He, Jianhua Wang\*, Decheng Wan

Computational Marine Hydrodynamics Lab (CMHL), School of Naval Architecture, Ocean and Civil Engineering,  
Shanghai Jiao Tong University, Shanghai, China

\*Corresponding Author: Jianhua Wang

### ABSTRACT

With the trend of increasing dimensions of large ships, especially for the ultra large container ship, the hydroelasticity of ship in waves become more and more important. The hydroelastic responses, such as springing and whipping, happen more frequently even in sea states that were not regarded as severe before. It is of great importance to estimate the wave and vibration induced loads of ships accurately. In the present work, a fluid-structure interaction (FSI) method is developed based on CFD-FEM method to predict the hydroelastic response of a 20000TEU container ship in waves. Fluid field is solved by RANS method with OpenFOAM. Structural vibration is represented by Timoshenko beam model and solved by Newmark-beta method. The springing response of container ships in different regular waves are calculated. The predicted results, including ship motions, vertical bending moment, are compared with the experimental results. and the present CFD-FEM solver is proved to be reliable in predicting hydroelastic response for ultra large container ship in waves.

**KEY WORDS:** Fluid-structure interaction, CFD-FEM method, springing response, ship hydroelasticity

### INTRODUCTION

With the trend of increasing dimensions of large ships, particularly ultra large container ships with their length reaching approximately 400m, the ships become more flexible. The hydroelastic responses, such as springing and whipping, happen more frequently even in sea states that were not regarded as severe before. In recent years, a few critical ship accidents due to fatigue cracks and structure failure caused by hydroelastic responses took place unexpectedly. Two severe accidents involving large container ships occurred: MSC NAPOLI in 2007 and MOL COMFORT in 2013 (Hirdaris et al., 2023), as shown in Fig. 1. Both vessels were reported to have failed in a hogging condition due to the collapse of the hull girder. These accidents have drawn attention from the governmental organization (IMO), classification association (IACS) and international technical committees, such as ITTC and ISSC. Now, a joint work group between ISSC and ITTC is also carrying out research on this important issue of springing and whipping responses of ultra large

container ship.



Fig. 1. MSC NAPOLI Accidents and MOL COMFORT Accidents

Because the mechanism of hydroelastic response is not clear at present, the traditional wave load theory which regards ship girder as rigid body can not accurately predict the hydroelastic response of ship. At present, many literatures have proposed that hydroelastic response has influence on fatigue strength, but no specific laws have been given. At present, the industry has paid much attention to the fatigue damage of structures caused by hydroelastic response, but this problem has not been taken into account in current ship codes. Therefore, the prediction of high-frequency fatigue damage caused by hydroelastic response accounts for the proportion of total fatigue damage and will be of great significance to the revision of wave load design formula in civil ship fatigue rules. In order to simulate the hydroelastic vibration of large ships and forecast the wave loads on ships accurately, it is more and more important to study the fluid-solid coupling of ship-sea structures.

There are many published papers on the theory of hydroelastic response prediction, such as Goodman (1970) and Hoffman (1976). Faltinsen (1982) carried out a detailed study on the elastic-vibration effect by simplifying the ship into a two-joint bending beam. Watanabe et al. (1999) used various non-linear programs to calculate the vertical bending moment of a container ship and made a comparison of the results. The results show that the results of linear prediction with different programs are more consistent in states with lower wave heights, but the results are quite different in states with higher wave heights because the impact of elastic vibration in states with higher wave heights on the vertical bending moment is greater. Different procedures have different ways of considering the elasticity of ships.

Malenica et al. (2006) applied a simplified beam model to the horizontal

bending and torsion and proposed a set of methods for predicting the two aspects of ships. This method can be used in the initial design stage of ships. The results of a barge example were analyzed by using the simplified beam model and the three-dimensional finite element model. It was found that the simplified beam model can get more accurate results. Kim et al. (2008) carried out research and Analysis on wave-induced vibration of ships under zero-speed inclined wave condition. The structure was solved by combining finite element model of beam and three-dimensional boundary element method. It differs from the previous constant panel method in that the pressure on each panel is no longer a fixed value but is related to the rate of change in the shape of the panel. In this way, the ship flutter in time domain and linear wave-induced vibration in frequency domain can be simulated.

Lakshmyarayanan et al. (2019, 2020) based on the combination of STAR-CCM+ and Abaqus, carry out the numerical simulation of two-way fluid-structure interaction for the elastic barge and S175 container ship. The Timoshenko beam model was adopted to establish the kinematic constraint relationship between the deformation of the beam joint and the deformation of the grid node on the hull surface, so as to realize the bending of the elastic hull. The numerical results were in good agreement with the experiment data. Jiao et al. (2021) proposed a CFD-FEA two-way coupling method for predicting the response of ships in regular waves. By comparing the results with experimental results, it is considered that the two-way coupling method can accurately simulate the green water loads and whipping and springing responses of the hull in waves. Show et al. (2022) presented a BEM-FEM method by combining a time-domain green function with Timoshenko beam structural dynamics. They predicted three container ships' responses in waves and results were validated by comparisons against a range of available experimental data.

To sum up, CFD-FEM approach is now becoming more and more popular in predicting ship slamming problems when encountering severe sea conditions. In the present work, a CFD-FEM solver is developed based on OpenFOAM to predict the hydroelastic responses of a 20000 TEU container ship at different wavelengths.

## NUMERICAL METHOD

### Governing Equations of Fluid

The flow is assumed to be incompressible, unsteady and viscous. The governing equation is Reynolds averaged Navier-Stokes equation which is presented as follows.

$$\frac{\partial u_i}{\partial x_i} = 0 \quad (1)$$

$$\frac{\partial u_i}{\partial t} + \frac{\partial}{\partial x_j} (u_i u_j) = -\frac{1}{\rho} \frac{\partial p}{\partial x_i} + \nu \frac{\partial}{\partial x_j} \left[ \frac{\partial u_i}{\partial x_j} + \frac{\partial u_j}{\partial x_i} \right] \quad (2)$$

where  $u(i=1,2,3)$  is the velocity component in the direction of the three axes of  $x$ ,  $y$ , and  $z$ ;  $x(i=1,2,3)$  is the coordinate component in the direction of the three axes of  $x$ ,  $y$ , and  $z$ .  $p$  is the pressure of the fluid;  $\rho$  is the density of the fluid;  $\nu$  is the kinematic viscosity coefficient of the fluid;  $t$  is the time.

In order to accurately capture the free surface when containership sailing in marine, this work use the volume of fluid (VOF) method to control the numerical spread. The equations can be expressed as:

$$\frac{\partial \alpha}{\partial t} + \nabla \cdot [(U - U_g)\alpha] + \nabla \cdot [U_r(1 - \alpha)\alpha] = 0 \quad (3)$$

where  $\rho$  is the fluid density,  $\alpha$  is the volume fraction and  $0 < \alpha < 1$ . The volume fraction  $\alpha$  can be expressed as:

$$\alpha = \begin{cases} 0 & \text{air} \\ 1 & \text{water} \end{cases} \quad (4)$$

At the same time, the fluid density  $\rho$  and the coefficient of dynamic viscosity  $\mu_{\text{eff}}$  can also be expressed by  $\alpha$ .

$$\rho = \alpha \rho_l + (1 - \alpha) \rho_g \quad (5)$$

$$\mu = \alpha \mu_l + (1 - \alpha) \mu_g \quad (6)$$

where the  $\rho_l$  and  $\mu_l$  represent the density and dynamic viscosity of water, the  $\rho_g$  and  $\mu_g$  represent the density and dynamic viscosity of air.

### Governing Equations of Structure

The Euler-Bernoulli beam model is used for structural solution. The structural dynamics control equation is:

$$[M][\ddot{x}] + [C][\dot{x}] + [K][x] = [F] \quad (7)$$

Where  $[M]$  is the structural mass matrix,  $[C]$  is the structural damping matrix,  $[K]$  is the structural stiffness matrix,  $[F]$  is the equivalent nodal force matrix, and  $[x]$  is the node displacement matrix.

The structural dynamics equations were solved by using Newmark- $\beta$  Methods. The displacement of the  $(i+1)$ th node can be calculated from the displacement, velocity and acceleration of the  $i$ th node.

$$\hat{K}x_{i+1} = \hat{F}_{i+1} \quad (8)$$

$$\hat{K} = K + \frac{1}{\beta(\Delta t)^2} M + \left( \frac{\delta}{\beta(\Delta t)} \right) C \quad (9)$$

$$\hat{F}_{i+1} = F_{i+1} + \left[ \frac{1}{\beta(\Delta t)^2} x_i + \frac{1}{\beta(\Delta t)} \dot{x}_i + \left( \frac{1}{2\beta} - 1 \right) \ddot{x}_i \right] M + \left[ \frac{\delta}{\beta(\Delta t)} x_i + \left( \frac{\delta}{\beta} - 1 \right) \dot{x}_i + \frac{\Delta t}{2} \left( \frac{\delta}{\beta} - 2 \right) \ddot{x}_i \right] C \quad (10)$$

Where  $\beta = 0.25$  and  $\delta = 0.5$ . For the Newmark- $\beta$  method,  $\beta$  and  $\delta$  can be varied to achieve the best stability and accuracy. When  $\delta \geq 0.5$  and  $\beta \geq 0.25(0.5 + \delta)$ , the integral format is unconditionally stable. When  $\beta = 0.25$  and  $\delta = 0.5$ , this method can give the most satisfactory accuracy.

### Coupling Method

The computational domain of the fluid-structure coupling problem includes the fluid domain and the solid domain. There is a common boundary between the two computing domains. For the interaction between incompressible fluid and elastic structure, the pressure acting on the structure surface from the flow field is generally used as the variable to solve the structural field, and the structural displacement is used as the variable to update and solve the flow field. Specifically, in the fluid mesh, the mesh on the hull surface will be divided into several groups along the direction of the ship, and these groups will correspond to the elements of the beam one-to-one, and the force of the corresponding beam element can be obtained by integrating the force of the fluid mesh in each group.

In the present study, the hydrodynamic forces and 6DoF motions are first calculated using in-house CFD solver naoe-FOAM-SJTU (Wang et al., 2019). Then the forces are applied to the hull girder as distributed forces on the Euler-Bernoulli beam model to calculate the structural response. So far, only weak coupling is used for the prediction of fluid structure interaction.

## NUMERICAL COMPUTATION

### Geometry Model

The geometry model of the containership is shown in Fig. 2, and the figure containership's principal dimensions in model scale are provided in Table 1.



Fig. 2. Geometry model of containership

Table 1. Main particulars of containership

Particulars	Symbols and units	Value
Length between perpendiculars	L (m)	7.816
Total width	B (m)	1.196
Fore Draft	T1 (m)	0.310
Aft Draft	T2 (m)	0.341
Depth	D (m)	0.46
Displacement	$\nabla$ (ton)	2.161

### Test Conditions and Numerical Settings

The conditions in this work are shown in Table 2.

Table 2. Test conditions

Conditions	Symbols and units	Value
Velocity	U (m/s)	0.8451
Wave-length	$\lambda/L$	0.8 0.9 1.0 1.1 1.2
Wave height	$H_s$ (m)	0.102
Wave direction	X (deg)	180

Because the container ship is symmetrical about the middle longitudinal section, the numerical calculation domain used in this work is the semi-ship calculation domain, which can greatly reduce the calculation cost and time. The preprocessing tools blockMesh and snappyHexMesh in OpenFOAM are used to generate mesh, blockMesh is used to generate background meshes, and snappyHexMesh is used to generate meshes around ship hull, refine locally, and add boundary layers. The computational domain size and grid information are shown in Fig. 3 and Fig. 4, respectively. Boundary conditions are shown in Table 3.

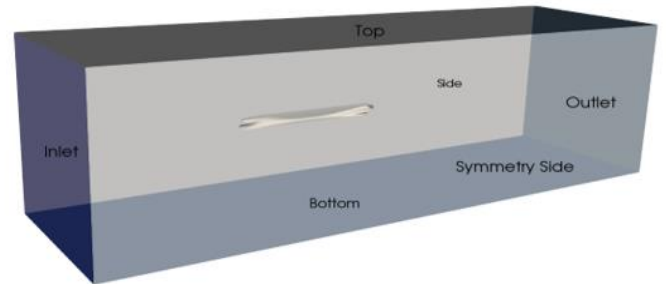
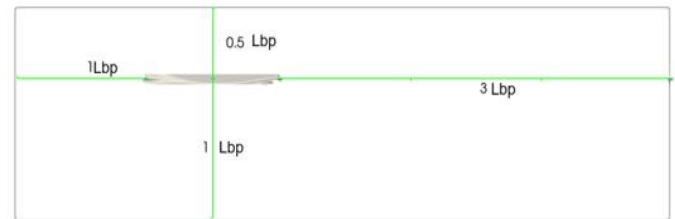


Fig. 3. Computational domain

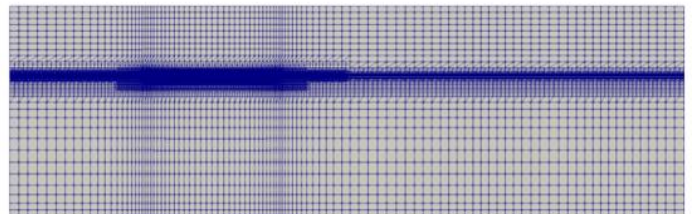
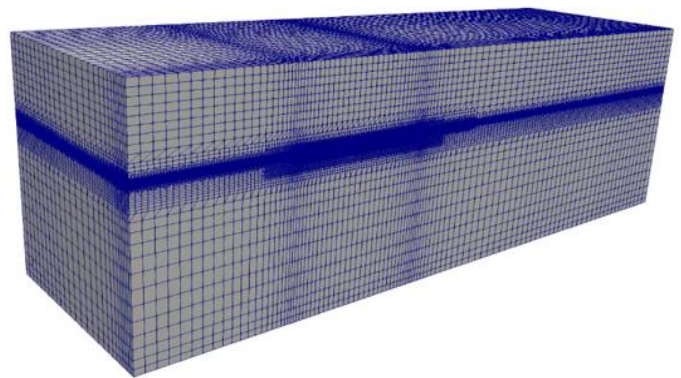


Fig. 4. Mesh distribution

In structural calculation, 100 elements are set up for hull girder. Fig. 5 shows the element division of hull girder. 10 segments are set in the experiment, and each segment was divided into 10 units in the numerical simulation, so as to set parameters such as cross-section area of hull girder to ensure identical with variable-section beam in experiment.

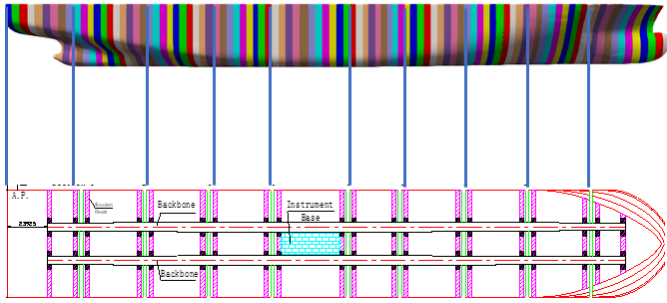


Fig. 5. Structure element distribution

Table 3. Boundary conditions

Boundary	Boundary conditions
Inlet	Velocity inlet
Top	Non-slip condition
Symmetry Side	Non-slip condition
Hull	Non-slip wall condition
Outlet	Pressure outlet

### Simulation Results and Discussions

Since regular head wave conditions are considered, only pitch and heave motions are released in the present numerical simulations. At the initial moment, the container ship is kept in a positive floating state, and the speed of the ship is replaced by the incoming speed of the water. Fig. 6 shows the situation of the ship's bow entering and leaving the water surface when  $\lambda/L=1$ . It can be seen that the free surface is broken and splashed at the time of the bow entering the water surface, but there is no green water in this condition.

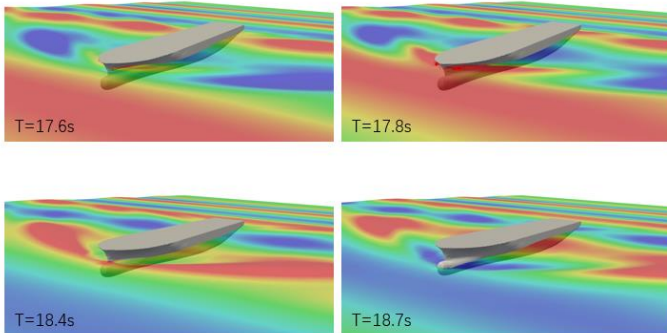


Fig. 6. Time instance of coupled CFD simulations showing bow emerging in and out of the water surface.

RAO value is calculated by averaging the peak to peak value of the last six stable periodic time signals, according to the  $\lambda/L$  draw response diagram. The comparisons of the pitch and heave of the container ship simulated by CFD with the experiment results are shown in the Fig. 7 and Fig. 8. The experiment results are from towing tank measurements from China Ship Scientific Research Center (CSSRC).

The pitch motion amplitude of the container ship is related to the  $\lambda/L$ . When the wavelength and the length of the ship become closer, the amplitude of pitch becomes smaller. The heave motion of container ships will increase with the increase of wavelength. The errors of pitch and heave motions of container ships between the CFD and the experiment results are 7.4% and 3.8% respectively. The numerical results are in good agreement with the test results, which shows that the use of this solver

can predict the heave and heave motions of container ships in waves well.

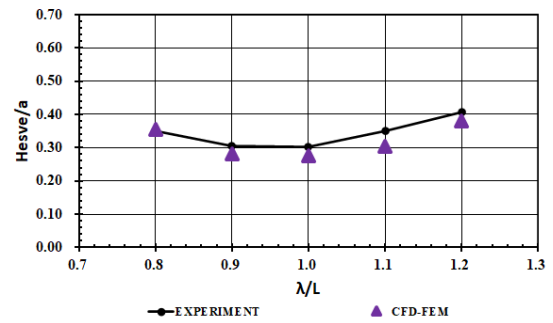


Fig. 7. Heave RAO plotted against  $\lambda/L$  for the simulations and the measurements.

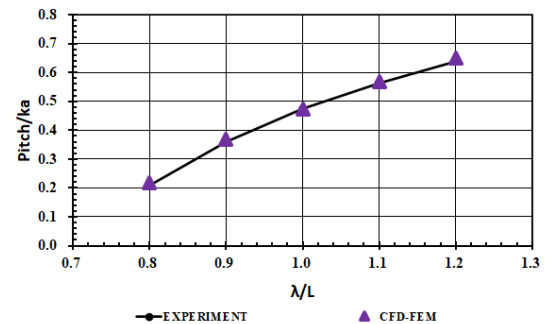


Fig. 8. Pitch RAO plotted against  $\lambda/L$  for the simulations and the measurements.

The following Fig. 9 contains the amplitude response operator (RAO) of the bending moment value in the midship with different wavelength length ratio. It can be seen that when the  $\lambda/L=0.9$ , the vertical bending moment amplitude at the midship position is the largest in CFD-FEM. When  $\lambda/L$  increases or decreases from 0.9, the vertical bending moment in the midship will gradually decrease. It is because when the length of the wave is close to the length of ship, the ship-wave matching resonance will occur and the bending of the hull is the most serious. Mid-vertical bending and mid-arch bending will occur in the wave. At this time, the vertical bending moment in the ship is the largest. When the difference between  $\lambda$  and  $L$  gradually increases, the deformation in the middle of the hull girder will be correspondingly reduced and the vertical bending moment in the ship will also be correspondingly reduced. However, in the results of numerical simulation, the maximum value of the vertical bending moment in the ship appears in the condition of  $\lambda/L=0.9$ . In experiment result, the vertical bending moment becomes the largest in the condition of  $\lambda/L=1$ . It can also be seen from Fig. 9 that in the numerical simulation, the variation of the vertical bending moment in the ship with the ratio of  $\lambda/L$  is significantly greater than the experiment results. The maximum error between the numerical simulation results and the experiment results can be up to 20.5%. Since the ship model is a large container ship, its hull girder is flexible. Therefore, the deformation of the hull will have a greater impact on the fluid field around the ship and the calculation of the vertical bending moment of the ship. Therefore, one-way coupling approach may lead to the discrepancies between the numerical simulation results and the experiment results.

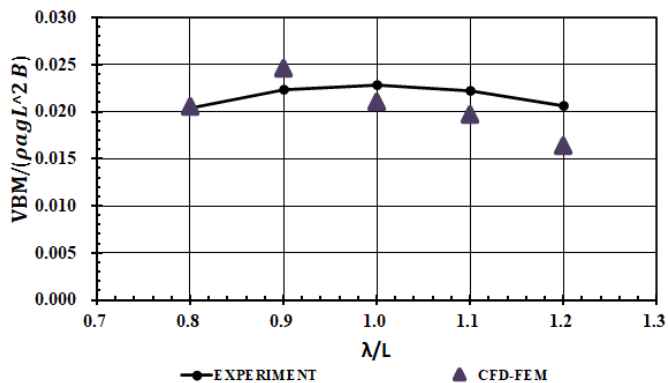


Fig. 9. VBM in amidship RAO plotted against  $\lambda/L$  for the simulations and the measurements.

Fig.10 shows the results obtained from coupling analysis time history of total VBM in midship with  $\lambda/L=1$ . It can be seen that in a wave period, the vertical bending moment of the ship has three peaks, which is different from the phenomenon that there is only one peak in a wave period in the history of the bending moment of the rigid ship, which indicates that the elasticity of the hull has a great impact on the response of the hull. Use band filter to extract  $\lambda/L=1$  wave frequency (first harmonic) and high frequency component (closer to 2-node wet frequency), as shown in the Fig.11, where 1\_LF represents low-frequency component, 1\_HF stands for high frequency component. It can be seen that the low-frequency component is the main component, which is mainly caused by the rigid motion of the hull, while the high-frequency component is about 13.6%, which is mainly caused by the vibration of the hull beam.

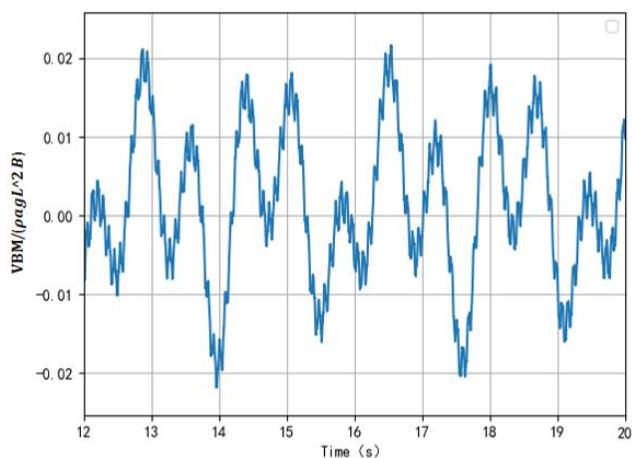


Fig. 10. Time history of VBM amidships computed when  $\lambda/L=1$

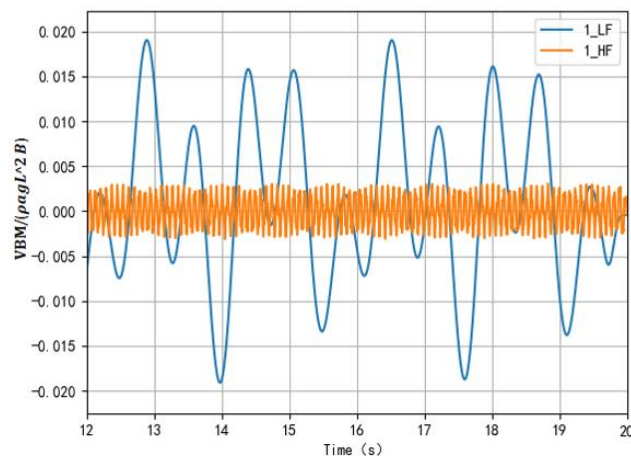


Fig. 11. Time history of frequency components in VBM amidships extracted using a band-pass filter when  $\lambda/L=1$ .

## CONCLUSION

Based on the in-house CFD-FEM solver, this paper simulates the responses of a 20000 TEU container ship in head seas condition. The simulation results are compared with the experimental results. Specific conclusions are as follows:

- Through numerical simulation based on the in-house CFD-FEM solver, the heave and pitch motions in different wavelengths are compared with the experiment results. It is found that the numerical simulation results are in good agreement with the experiment data. The agreement between the two results shows that this CFD-FEM solver can be used to predict the motion of large container ships in waves and provide data support for the design process of container ships.
- Based on the numerical simulation by our internal CFD-FEM solver in one-way coupling, the magnitude of the vertical bending moment in the mid of container ship and its variation trend with  $\lambda/L$  are close to the experiment values, which indicates that the CFD-FEM solver can be used to predict the extreme value of the vertical bending moment in the container ship.

The present work only considers the head sea conditions, future work will conduct oblique wave conditions and study the wave direction influences on the hydroelastic performance. The two-way coupling method will also be studied to better predict the vertical bending moment.

## ACKNOWLEDGEMENTS

This work was supported by the National Key Research and Development Program of China (2019YFB1704200), the joint project with CSSRC, to which the authors are most grateful.

## REFERENCES

- Faltinsen, O (1993). "Sea loads on ships and offshore structures." *Cambridge university press*.
- Goodman, RA (1971). "Wave-excited main hull vibration in large tankers and bulk carriers," *Naval Architect*.
- Hirdaris, S, Parunov, J, Qui, W, Iijima, K, Wang, X, Wang, S, ... and Soares, CG (2023). "Review of the uncertainties associated to hull girder hydroelastic response and wave load predictions." *Marine Structures*, 89, 103383.
- Hoffman, D, and Van Hooff, RW (1976). "Experimental and theoretical

evaluation of springing on a great lakes bulk carrier,” *Int Shipbuilding Progress*, 23(262), 173-193.

Jiao, J, Huang, S, Wang, S, and Soares, CG (2021). “A CFD–FEA two-way coupling method for predicting ship wave loads and hydroelastic responses.” *Appl Ocean Res*, 117, 102919.

Kim, Y, and Kim, Y (2008). “Analysis of springing effects on floating barges in time domain by a fully coupled hybrid BEM-FEM.” *Proc. 23rd Int. Workshop on Water Waves and Floating Bodies IWWWFB*, Jeju, Korea.

Lakshmyanarayanan, PA, and Temarel, P (2019). “Application of CFD and FEA coupling to predict dynamic behaviour of a flexible barge in regular head waves.” *Marine Structures*, 65: 308-325.

Lakshmyanarayanan, P. A., and Temarel, P (2020). “Application of a two-way partitioned method for predicting the wave-induced loads of a flexible containership.” *Appl Ocean Res*, 96,102052.

Lakshmyanarayanan, PAK, and Hirdaris, S (2020). “Comparison of

nonlinear one-and two-way FFSI methods for the prediction of the symmetric response of a containership in waves.” *Ocean Eng*, 203, 107179.

Malenica, S (2006). “An efficient hydroelastic model for wave induced coupled torsional and horizontal ship vibrations.” *Proc of the 21st IWWWFB*, Loughborough, UK.

Show, TK, Hirdaris, S, and Datta, R (2022). “A Fully Coupled Time-Domain BEM-FEM Method for the Prediction of Symmetric Hydroelastic Responses of Ships with Forward Speed.” *Shock and Vibration*, 4564769.

Watanabe, I, and Soares, CG (1999). “Comparative study on the time-domain analysis of non-linear ship motions and loads.” *Marine Structures*, 12(3): 153-170.

Xing, JT (2019). “Fluid-Solid interaction dynamics: Theory, variational principles, numerical methods, and applications.” *Academic Press*.